

This is an Open Access document downloaded from ORCA, Cardiff University's institutional repository:<https://orca.cardiff.ac.uk/id/eprint/93897/>

This is the author's version of a work that was submitted to / accepted for publication.

Citation for final published version:

Kusche, Juergen, Eicker, Annette, Forootan, Ehsan , Springer, Anne and Longuevergne, Laurent 2016. Mapping probabilities of extreme continental water storage changes from space gravimetry. *Geophysical Research Letters* 43 (15) , pp. 8026-8034. 10.1002/2016GL069538

Publishers page: <http://dx.doi.org/10.1002/2016GL069538>

Please note:

Changes made as a result of publishing processes such as copy-editing, formatting and page numbers may not be reflected in this version. For the definitive version of this publication, please refer to the published source. You are advised to consult the publisher's version if you wish to cite this paper.

This version is being made available in accordance with publisher policies. See <http://orca.cf.ac.uk/policies.html> for usage policies. Copyright and moral rights for publications made available in ORCA are retained by the copyright holders.



¹ Mapping probabilities of extreme continental water ² storage changes from space gravimetry

J. Kusche¹, A. Eicker¹, E. Forootan^{1,2}, A. Springer¹, and L. Longuevergne³

Corresponding author: J. Kusche, Institute of Geodesy and Geoinformation, University of Bonn, Nussallee 17, D-53115 Bonn, Germany. (kusche@uni-bonn.de)

¹Institute of Geodesy and Geoinformation, University of Bonn, Bonn, Germany.

²School of Earth and Ocean Sciences, Cardiff University, Cardiff, UK.

³CNRS, Geosciences Rennes, University of Rennes 1, Rennes, France.

Key Points.

1. From 12 years of GRACE data, we derive statistically robust 'hotspot' regions of high probability of peak anomalous water storage and flux.

2. Comparison to ERA-Interim reanalysis reveals good agreement of these regions to GRACE, with most exceptions located in the Tropics.

3. Provided GRACE will be succeeded in time by GRACE-FO, by around year 2020 we will be able to detect changes in the frequency of peak total flux.

3 Using data from the Gravity Recovery and
4 Climate Experiment (GRACE) mission, we
5 derive statistically robust 'hotspot' regions of
6 high probability of peak anomalous – i.e. with
7 respect to the seasonal cycle – water storage
8 (of up to 0.7 m one-in-five-year return level)
9 and flux (up to 0.14 m/mon). Analysis of, and
10 comparison to, up to 32 years of ERA-Interim
11 reanalysis fields reveals generally good agree-
12 ment of these hotspot regions to GRACE re-
13 sults, with most exceptions located in the Trop-
14 ics. A simulation experiment reveals that dif-

15 ferences observed by GRACE are statistically
16 significant. Further error analysis suggests that,
17 provided we will have a continuation of GRACE
18 by its follow-up GRACE-FO, we will likely be
19 able around year 2020 to detect temporal changes
20 in the frequency of extreme total fluxes (i.e.
21 combined effects of mainly precipitation and
22 floods) for at least one tenth to one fifth of the
23 continental area.

1. Introduction

24 Due to its memory effect, terrestrial water storage contains information on antecedent
25 rainfall and runoff conditions that, to some extent, control future drought and flood
26 occurrence and severity. However, at the time of writing, the NASA/DLR GRACE twin-
27 satellite mission represents the only platform that observes terrestrial water storage with
28 global coverage. GRACE has provided an unprecedented record of more than 14 years
29 of monthly terrestrial water storage anomaly maps. The GRACE satellites show signs of
30 ageing, but with its successor GRACE-FO set for launch in 2017 [*Flechtner et al.*, 2016],
31 it appears possible that we will soon have an almost uninterrupted observational record
32 of terrestrial water storage over three decades. The primary observable of GRACE, time-
33 variable changes in the Earth's geopotential measured via precise intersatellite ranging,
34 has provided a new view on the ongoing patterns of mass redistribution at the planet's
35 surface, in particular related to the terrestrial and oceanic hydrological cycle.

36 Several researchers quantified the variability of water storage in form of groundwater, soil
37 moisture, and surface water [*Forootan et al.*, 2014], snowpack and ice [*Velicogna et al.*,
38 2014], and mass-driven sea level [*Rietbroek et al.*, 2016], on different timescales from in-
39 terannual to days. Observed variability in groundwater storage has been attributed to
40 episodic events such as droughts and floods, to 'natural' variability related to modes of
41 the climate system [*Phillips et al.*, 2012], and to anthropogenic effects such as depletion
42 [*Döll et al.*, 2014] and land use change.

43 *Ogawa et al.* [2011] have shown how GRACE data can be related to total terrestrial water
44 flux, the sum of precipitation, evapotranspiration, and runoff, and *Springer et al.* [2014]

45 suggested its use to validate the water cycle in atmospheric reanalyses. In these applica-
46 tions, numerical differentiation schemes are applied to total water storage time series in
47 order to derive flux. At longer time scales, anomalies of total flux with respect to a mean
48 state can be linked to the sum of (i) modifications of the land boundary conditions and
49 the resulting climate forcing, (ii) the direct and indirect impact of anthropogenic activ-
50 ities, and (iii) the hydrological response of the system [*Eicker et al.*, 2016]. Important,
51 at shorter time scales and at grid scale, GRACE data relate to lateral water redistribu-
52 tion: water storage increase (flux has a positive sign) corresponds to precipitation plus
53 upstream river flow, while storage decrease (flux has a negative sign) corresponds to evap-
54 otranspiration plus river discharge. However, inferring lateral transports from GRACE
55 is difficult since month-to-month variability in GRACE data is contaminated by stronger
56 noise and limited in spatial resolution, when compared to longer timescales.

57 Estimating the frequency or probability of future events based on time-limited records
58 represents an established concept in hydrology and hydrological engineering (e.g. *Beard*
59 [1962], *Stedinger et al.* [1992]). Drought and flood indicators can be expressed as per-
60 centiles in reference to their historical frequency of occurrence. For example, the U.S.
61 Drought Monitor combines several short-term and long-term indices and indicators in
62 this way for each location and time of year. Since only little information on deep soil
63 moisture and groundwater enters common drought indices, GRACE data are being as-
64 similated in the Catchment Land Surface Model, and assimilated fields are converted into
65 soil moisture and groundwater percentiles [*Houborg et al.*, 2012].

66 Few studies so far (e.g. *Moore and Williams* [2014], *Humphrey et al.* [2016]) have at-

67 tempted to look directly at the statistical behaviour of 'anomalous' GRACE signals, i.e.
68 beyond the dominating seasonal cycle and beyond episodic drought and flood events, and
69 no study is known to us that quantifies occurrence frequency and expected return levels
70 of such changes in a probabilistic sense.

71 In particular interesting would be, in the light a hypothesized intensification of the wa-
72 ter cycle (*Huntington* [2006], or [*Durack et al.*, 2012]), whether and if, after what time,
73 changes in the occurrence frequency of extremes in storage and flux, including floods and
74 droughts, can be observed with space gravimetry. In a probabilistic view, changes in the
75 mean and variance of the distribution underlying a climate variable affect the severity
76 and occurrence frequency of extremes [*Folland et al.*, 2001]. Return times of events of a
77 given magnitude, or return levels for a given return time as considered here, are sensitive
78 indicators to increases in magnitude in the tails of the underlying distribution [*Allen and*
79 *Ingram*, 2002]. For example, the CMIP5 analysis by *Yoon et al.* [2015] projects an in-
80 crease in the sliding-window variance of California top-1m soil moisture that equates to
81 an increase of intense droughts and excessive floods by at least 50% towards the end of
82 the twenty-first century. Validating such studies using GRACE/GRACE-FO would be of
83 tremendous significance.

84 Here, we analyse annual peak high and low levels of water storage and in storage change
85 (total flux), observed by GRACE, for their recurrence frequency and levels in a probibilis-
86 tic framework. Recurrence frequency and return level are equivalent once the underlying
87 distribution is known, so we express all findings as return levels. We outline hotspot re-
88 gions where large anomalies are to be expected, which differ, to some extent, from what

89 is expected based on 32 years of ECMWF ERA-Interim reanalysis. Based on a realistic
90 simulation, we then discuss the probability of detecting temporal changes in recurrence
91 frequency of total water flux with the future combined GRACE/GRACE-FO data record.

2. Data and methods

92 Total water storage (TWS) represents aggregated variations in the terrestrial water
93 content with respect to a long-term mean; thus reflecting the combined effect of changes
94 in groundwater volume, soil moisture, root and canopy water content, and lake, river
95 and reservoir levels. We use GRACE data to derive TWS as follows: Monthly spheri-
96 cal harmonic coefficients (University of Texas, release 5) for the 2003.0-2015.0 timespan,
97 augmented by geocenter, c_{20} , and glacial isostatic adjustment (GIA) corrections and decor-
98 related/smoothed through the DDK3 method as in *Eicker et al.* [2016], are mapped to 1°
99 grids. Finally, in order to focus on departures from the large average seasonal water stor-
100 age modes, we first remove a six-parameter model (mean, rate, annual and semi-annual
101 waves), and then, subsequently, the monthly residual TWS climatology from the grids.

102 The instantaneous rate of change of TWS corresponds, according to mass conservation,
103 to the sum of precipitation, evapotranspiration and runoff, and we denote this quantity
104 as total water flux (TWF) here. From the GRACE coefficients, TWF grids are derived
105 following methods outlined in *Eicker et al.* [2016]. Since TWF exhibits more noise due to
106 temporal differentiation, we chose to apply slightly more aggressive spatial filtering (DDK2)
107 as compared to TWS grids.

108 It is not clear whether any current hydrological or land surface model captures the full

109 storage capacity in all soil and groundwater layers, and lends itself for providing a reference
110 for GRACE-derived extreme TWS and TWF under either stationarity or non-stationarity
111 assumptions. In this work, both for comparison and multi-decadal simulation purposes,
112 TWF grids are derived directly from ERA-Interim reanalysis fields [Dee *et al.*, 2011] of
113 precipitation, evapotranspiration and runoff. We realize that limitations of the under-
114 lying land surface model (H-TESSSEL) exist, but results in *Eicker et al.* [2016] suggest
115 that ERA-Interim and GRACE data fit well at shorter timescales. To enforce spectral
116 consistency, these fields are first converted to spherical harmonic representation, filtered
117 using the same procedures as with GRACE, and converted back to grids as in *Eicker et al.*
118 [2016].

119 From this point on, our method is as follows (see supporting information): We decimate
120 all grid time series first to annual maximum and minimum anomalous storage and flux,
121 and compute mean, standard deviation and skewness (up to 2.6-2.9) for these peak series.
122 A Generalized Extreme Values (GEV) distribution is then fitted using a moment method
123 [Martins and Stedinger, 2000], and return levels (i.e. expected maximum or minimum
124 after N years) are computed. This has the advantage that occurrence frequencies can be
125 represented through a single, physically interpretable value (the N -year return level in m
126 or m/mon) per grid point. Since the GRACE record is rather short compared to precipi-
127 tation, discharge or sea level data where GEV analysis is common, we restrict ourselves in
128 this study to one-in-five-year return levels, and no attempt is made to extrapolate return
129 level curves to more infrequent extremes.

3. Probabilities of anomalously high or low water storage

130 Following this approach, Fig. 1 illustrates return levels of annual anomalously high (a)
131 and low (b) water storage from GRACE, with respect to the monthly TWS climatology.
132 Expected one-in-five-year peak water levels reach up to 0.70 m, with dominating regions
133 being the Central Amazon and the Mississippi (related to catastrophic 2011 floods) basins,
134 and a range of regions at the 0.2 - 0.4 m level; such as the South America Parana basin,
135 Central Africa (including the Zambezi), India, Northern Australia, Turkey, and North-
136 East China (it is important to understand that expected N -year levels can be larger than
137 those actually observed within any N -year period). Measured by the latitude-weighted
138 RMS, land-averaged return levels amount to 0.14 m. As an aside, we note that one-in-
139 ten-year levels are generally found about 25% larger than one-in-five year levels.

140 It must be understood that, at GRACE temporal and spatial resolution, hydro-
141 meteorological extreme events are difficult to relate to common flood or rainfall peak
142 levels or return intervals. For example, the 2011 Mississippi 500-year flood inundated an
143 area of several thousand km² by the order of meters, as a result of rainfall rates of 50
144 cm per week but concentrated within few days. Though GRACE results are typically ex-
145 pressed in metric 'equivalent water height', due to its measurement principle the mission
146 observes water mass (or 'equivalent volume') which is difficult to scale to observable water
147 levels. As a result, GRACE-derived extreme events always refer to monthly large-scale
148 averages and may miss, or average out, 'real' extreme events that are focused in space
149 and time by nature.

150 In contrast to annual maxima, one-in-five-year levels of exceptional low (i.e. below cli-

matology) water storage are found reaching 0.55 m in the Amazon, and on average over
land masses, less than 0.14 m. It is interesting to note that extreme levels in TWS are
not symmetric; some regions affected by floodings (e.g. Mississippi basin, Lake Victoria)
feature prominently in Fig. 1.a while some others show up only (Amazonas river mouth)
in Fig. 1.b, but overall the maps are quite similar. 14-year minimum TWS events have
been analysed in *Humphrey et al.* [2016], and their Fig. 14 of maximum average storage
deficit and year of maximum resembles our Fig. 1.b. This confirms that levels of high
probability of low water storage in our Fig. 1.b are typically related to the occurrence of
two or three strong droughts (some of which may not have been described in literature,
Humphrey et al. [2016]).

As expected, these hotspot regions of extreme annual anomalous storage broadly corre-
spond to regions where seasonal water storage amplitudes are large (see Fig. S1), but they
also reflect that GRACE picks up anomalous floods and droughts for Southern Australia,
the Parana basin (where the large groundwater response to climate variability was shown
in *Chen et al.* [2010]), or North East China regions where the annual signal is less promi-
nent. On the contrary, Fig. 1 does not prominently feature part of the Amazon, Alaska
coastal glaciers, and the Ganges-Brahmaputra delta where surface or snow-equivalent wa-
ter loads are huge but mostly follow the seasonal cycle (Fig. S1).

Figure 1 (c, d, g, and h) show time series (black dots), annual maximum TWS levels (red
dots), observed frequency of maximum TWS (red bars) and the fitted GEV distribution
(grey) for the two locations Central Amazon (c,d), Parana (g, h) indicated in Fig. 1 (a),
while figures on the right-hand side show the same for minimum TWS levels (Cuvelai-

173 Etosha e, f, Northern Australia i, j). Locations have been chosen to display different
174 behaviour: Central Amazon where annual signals are among the largest on Earth, with
175 a wide spread of both annual maxima and minima of anomalous TWS, while for the
176 Cuvelai-Etosha basin [Eicker *et al.*, 2016] a multiannual oscillation appears to be present.
177 For the Parana basin, again the seasonal signal is weak but extreme levels peak every two
178 to three years, likely related to ENSO (*Chen et al.* [2010], *Phillips et al.* [2012], *Eicker*
179 *et al.* [2016]). We note that, with the exception of the Central Amazon location, the GEV
180 distribution appears quite suitable for fitting to observed extreme levels of storage. As
181 will be shown later, our GEV fits are less sensible with respect to record length compared
182 to, e.g. Gaussian fits.

4. Probabilities of anomalous increase or decrease of water storage

183 Analysis of the time-differentiated GRACE record reveals a number of regions of in-
184 creased probability of maximum (Fig.2.a) and minimum (Fig.2.b) water flux that broadly
185 correspond to those of anomalous TWS but in general follow rainfall patterns such as
186 the monsoon. One-in-five-year levels of annual peak flux (Fig.2.a) amount up to 0.14
187 m/mon for the Central Amazon region, with an overall land-average weighted RMS of
188 0.033 m/mon. We remind that annual extremes in TWF relate to the fastest increase
189 (linked to extreme precipitation) or decrease of total water storage per given year; and
190 peak maxima in the figures have to be interpreted as levels of storage increase or decrease
191 that statistically occur once every five year. Peak one-in-five year decrease (Fig.2.b)
192 reaches up to 0.14 m/mon, with a land-average RMS of 0.031 m/mon.

193 In ERA-Interim (Fig.2.c), tropical precipitation extremes dominate total flux and con-

194 tribute to one-in-five-year maximum levels up to 0.31 m/mon over Tropical Northern
195 Australia and South-East Asia, with RMS close to 0.040 m/mon. Minimum levels (Fig.2.c)
196 are up to 0.27 m/mon, land-averaged to RMS 0.036 m/mon. In fact, ERA-Interim iden-
197 tifies many regions outside the Tropics that closely correspond to GRACE-derived ex-
198 treme levels, with some exceptions (Southern Europe, US/Canada West coast, East Eu-
199 rope/Russia). Overall, we find an average difference between GRACE-derived TWF and
200 ERA-Interim reanalysis fields of only RMS 0.023 m/mon (max) and 0.021 m/mon (min).
201 *Humphrey et al.* [2016] found significant positive correlation between GRACE high-
202 frequency anomalies and ERA-Interim precipitation over many regions, that we identify
203 here as having high probability of maximum water flux: the Amazon and Parana basins,
204 Northern Australia, South/Central Africa, Northern India, South-East Europe, parts of
205 the U.S.. This supports our hypothesis that extreme levels of TWS increase (positive
206 TWF) are likely driven by precipitation.

5. Stationarity with respect to climate modes: ENSO

207 It is possible that our results are influenced by the occurrence of climate modes within
208 the analysis time frame. In fact, *Phillips et al.* [2012] and *Eicker et al.* [2016] have shown
209 that GRACE-derived water storage is correlated with ENSO, and other authors have
210 identified correlations e.g. with the Pacific Decadal Oscillation (PDO, e.g. *Seoane et al.*
211 [2013]). While these studies generally focused on identification of modes and problems
212 in estimation of trend and accelerations, we here focus on the imprint of ENSO on the
213 occurrence probability of extreme storage and flux.

214 In what follows, we repeat our previous experiments but we exclude either (1) years 2003,
215 2009, and 2010, or (2) 2007, 2008, 2010 and 2011 from our analysis. These years were,
216 according to the Ocean Niño Index (ONI, a three-month running mean of sea surface
217 temperature anomalies in the Niño3.4 region) categorized as (1) moderate or stronger El
218 Niño years ($\text{ONI} > 1$) or (2) moderate or stronger La Niña years ($\text{ONI} < -1$).

219 Results are shown in Fig. S2, and can be compared to Fig.1 which shows return levels
220 derived from the full time series including ENSO years. We find that, overall, our results
221 are surprisingly robust. Largest differences can be observed for South America. In case
222 of (1), excluding El Niño years, maximum one-in-five-year water levels are reduced from
223 0.70 m (full 12-year period) to 0.50 m with land RMS 0.013 m, while for (2) excluding
224 La Niña years leads to up to 0.53 m with RMS 0.014 m. Yet, removing El Niño years
225 does not lead to a general smoothing, and for some regions one-in-five-year levels slightly
226 increase. In contrast, minimum five-year water levels (0.55 m for 12-year period) increase
227 by (1) removing El Niño years to up to 0.65 m with RMS 0.014 m, while for (2) excluding
228 La Niña years leads to up to 0.63 m with RMS 0.013 m.

229 Results for total flux (not reported here) point in the same direction. In line with expecta-
230 tions, we conclude that ENSO, to some extent, influences extreme high water volumes
231 and less so extremely low levels (storage deficit events). It is also interesting to note that
232 El Niño and La Niña do not appear to have a symmetric effect on water surplus; although
233 due to the reduced sample size such comparisons are problematic and need to be repeated
234 once we have longer data records.

6. Detecting an intensification from a future combined GRACE and GRACE-FO record

235 With 14 years of GRACE data at the time of writing, and the GRACE Follow-On
236 mission (GRACE-FO) on track for launch in late 2017, it is reasonable to ask whether,
237 and after what time, a continuous multi-decadal data set of TWS and TWF will enable
238 us to detect temporal changes in the frequency of extreme water storage and water flux
239 events. In order to answer this question, we conduct a twin experiment: (1) We derive
240 the occurrence frequency of peak total water flux in ERA-Interim, when analyzed over
241 varying time frames from 32 years to 12 years, all ending January 2015. (2) We create
242 a synthetic, composite 32-years GRACE/GRACE-FO data set which is then analyzed
243 for peak TWF frequency over varying analysis intervals. This data set is derived from
244 the 'truth' ERA-Interim data by adding realistic, spatially anisotropic GRACE-errors.
245 In a conservative approach, we assume that GRACE-FO will have the same error char-
246 acteristics as GRACE (both GRACE and GRACE-FO errors are synthesized from fully
247 populated, monthly covariance matrices from real-data GRACE analysis over 2013 and
248 2014, as in *Landerer and Swenson [2012]*, but in random permutations over all 32 years).

249 In Fig. 3, we represent ERA-Interim-derived one-in-five-year peak water flux (left) and
250 the same statistics derived from synthetic GRACE/GRACE-FO (i.e. 'GRACE-perturbed'
251 ERA-Interim, Fig. 3 right), for 2003.0-2015.0 (top), 1991.0-2015.0 (center), and 1983.0-
252 2015.0 (bottom). All results are summarized in Table 1.

253 Differences between ERA-Interim peak TWF return levels over differing time spans, yet
254 referring to the same seasonal model, are small (cf. Table 1) but can be identified for

255 some regions (Orinoco basin, North-West India, Siberia). Such differences may occur due
256 to either problems in fitting the GEV distribution to small samples (comparing moment
257 and maximum likelihood (ML) estimation, or using the information matrix from the ML
258 approach [*Hosking, 1985*], suggests that 1σ values may be at the 0.01 - 0.02 m/mon level
259 from 12 years) or owing to real nonstationarity. But in our twin experiment we will as-
260 sume they represent the 'target signal' to be detected from the gravity mission records. As
261 expected, differences grow with decreasing analysis window. As a reference, for the same
262 12-year period for which we analysed real GRACE data, reanalysis-derived return levels
263 differ from those derived from 32 years by about 0.01 m/mon RMS and up to 0.09 m/mon
264 for the above mentioned regions. We note that it is of course possible that ERA-Interim
265 fails to capture real nonstationarity; in this case our GRACE/GRACE-FO simulation is
266 biased towards stationarity and conclusions on detectability may be too conservative.

267 Differences between one-in-five-year levels of peak TWF from simulated GRACE/GRACE-
268 FO data and the corresponding 'truth' ERA-Interim derived levels (right column in Table
269 1) vary from 0.007 m (32 years) to 0.011m (8 years); they depend on the data record
270 length but much less compared to Gaussian statistics such as applied in trend estimates.
271 Our twin experiment simulates that for the 12 year period analysed in this study from
272 real GRACE data, average RMS errors may be slightly above the 0.01 m level. In fact,
273 GRACE-like errors amplify near-zero peak levels over the Sahara desert (Fig. 3 b, d, f)
274 to about 0.02 m/mon which is almost exactly what we observe from the real GRACE
275 data (Fig. 2 a and b); the visual correspondence is striking, suggesting that our error
276 model may be quite close to the real noise. With the above, we can conclude that we find

277 ERA-Interim return levels above the noise level for nearly 90% of the total land area.

278 Finally, the RMS fit of GRACE/GRACE-FO peak levels from differing analysis windows
279 to the 32-year ERA-interim five-in-one-year return levels (middle column in Table 1) sug-
280 gest that temporal variability (or sampling error) of 'true' water flux and the effect of
281 GRACE errors add up virtually independent. This metric tells how good the satellite-
282 derived return levels from limited observational records would reconstruct 'true' return
283 levels under the assumption of stationarity.

284 The main conclusion from the twin experiment is that GRACE/GRACE-FO errors will
285 allow to derive return level statistics for water flux extremes at the 0.010 - 0.012 m/mon
286 land average error level within a 12 year temporal window (Table 1), only slightly less
287 accurate from 8-year windows, and more accurate down to 0.007 m/mon from 32 years.
288 In the light of our 12-year comparison of GRACE and ERA-Interim discussed in the pre-
289 vious section, this means that the differences observed by GRACE (Fig. 3 (a) vs. (c)
290 and (b) vs. (d)) exceed a noise level of 0.01 m/mon for about 40% of the land area (and,
291 conservatively, a noise level of 0.03 m/mon for still more than 9 % of the area).

292 This suggests that we apply a moving-window approach to a near-future GRACE/GRACE-
293 FO time series in order to isolate temporal changes in extreme water flux frequency. Our
294 error estimates can be compared against such changes in the ERA-Interim record, to
295 understand for which part of the landmass changes would be detected with statistical
296 significance. Yet, identifying such an 'intensification', leading to changes in the mean,
297 variability, or skewness of extremes and therefore to a change in e.g. one-in-five-year lev-
298 els, requires to contrast a certain window against a reference period of at least the same

299 duration. With this in mind, we deduce that for a 24-year data record with two 12-year
300 windows (i.e. corresponding to 2027, likely within the GRACE-FO lifetime), we could
301 have detected about 13 - 18% of the frequency changes in ERA-Interim (this is the share
302 of land area where changes exceed the noise). Surprisingly, for a 32-year data record,
303 divided into two windows each of the about the lifetime of GRACE, only for 10 - 16 % of
304 area such changes in ERA-Interim would be detected; this is since the longer timeframe
305 despite allowing for better GEV fitting tends to temporally average out changes in peak
306 frequency. On the contrary, our results suggest that already for a 16-year record (i.e.
307 2019) for 13 - 21 % of land area those changes in frequency that were captured in the
308 recent 8-year period in ERA-Interim with respect to the previous one would be detectable.

7. Conclusions

309 Climate variability as well as a range of direct and indirect anthropogenic modifications
310 of the water cycle cause land-atmosphere water fluxes and surface runoff to depart from
311 the regional climatology on a range of timescales. Such anomalous total water flux and
312 total water storage signals can be observed with the GRACE satellite mission and, with
313 its successor GRACE-FO hopefully launched in 2017, we may have soon a multi-decade
314 observational record that can be used to inform model simulations.

315 Here we have focused on the occurrence of extreme, annual maximum or minimum anoma-
316 lous fluxes and storages in the GRACE record. From 144 months of GRACE data, we
317 quantify and map return levels (expected anomalous flux or storage once in N years)
318 of these extremes, with good statistical significance. We find that most hotspot regions
319 correspond to regions of known large storage amplitudes due to groundwater variability

320 or seasonal flooding or inundation, but the situation is more complex and not symmetric.
321 Few studies so far have aimed at lateral water redistribution using GRACE due to its
322 comparably low resolution, but here we show that this is largely possible when focusing
323 on extreme events.

324 The current GRACE data set has been used before to isolate and study the response of
325 total water storage and of groundwater and river discharge to extreme events such as heat-
326 waves and heavy-precipitation years. Yet it is too short to derive conclusions on changes
327 in the probability of such events. But provided the GRACE mission will be succeeded in
328 time by GRACE-FO, we conclude that around year 2020 we will be able to detect changes
329 in the frequency of extreme total fluxes for at least one tenth to one fifth of the continental
330 area, when assuming the magnitude of such changes corresponds to what we observed in
331 the ERA-Interim reanalysis over the past decades. We anticipate that such changes may
332 occur along with an intensified water cycle due to global warming as the combined effects
333 of precipitation and floods. Yet, there is no consensus on what exactly may happen in
334 the future, and where, and we suggest that a combined GRACE/GRACE-FO record may
335 provide a useful additional observational data sets in order to test hypotheses regarding
336 the changing water cycle.

337 **Acknowledgments.** The University of Texas GRACE solutions are available via the
338 GFZ Potsdam Information Systems and Data Center (ISDC, isdc.gfz-potsdam.de) as
339 well as the JPL Physical Oceanography Distributed Active Archive Center (PODAAC,
340 www.grace.jpl.nasa.gov). The European Center for Midrange Weather Forecasting pro-
341 vided the ERA-Interim data, which are publicly available.

References

- 342 Allen, M. and W. Ingram, Constraints on future changes in climate and the hydrologic
343 cycle. *Nature*, *419*, 224-229
- 344 Beard, L. (1962), Statistical methods in hydrology. *U.S. Army Corps of Engineers*, Sacra-
345 mento, CA
- 346 Chen, J.L., C. Wilson, B. Tapley, L. Longuevergne, Z. Yang, and B. Scanlon (2010),
347 Recent La Plata basin drought conditions observed by satellite gravimetry, *J. Geophys.*
348 *Res. (Atmospheres)*, *115*, D22108
- 349 Dee, D.P., and 35 authors (2011), The ERA-Interim reanalysis: configuration and perfor-
350 mance of the data assimilation system, *Q. J. R. Meteorol. Soc.*, *137*(656), 553-597
- 351 Döll, P., H. Müller Schmied, C. Schuh, F. T. Portmann, and A. Eicker (2014), Global-scale
352 assessment of groundwater depletion and related groundwater abstractions: Combining
353 hydrological modeling with information from well observations and GRACE satellites,
354 *Water Resour. Res.*, *50*, 56985720
- 355 Durack, P., S. Wijffels, and R. Matear (2012), Ocean salinities reveal strong global water
356 cycle intensification during 1950 to 2000, *Science*, *336*(6080), 455-458
- 357 Eicker, A., E. Forootan, A. Springer, L. Longuevergne, and J. Kusche (2016), Does
358 GRACE see the terrestrial water cycle 'intensifying'?, *J. Geophys. Res. (Atmospheres)*,
359 *121*, 733–745.
- 360 Flechtner, F., K.-H. Neumayer, C. Dahle, H. Döbslaw, E. Fagiolini, J.-C. Raimondo, and
361 A. Güntner (2016), What can be expected from the GRACE-FO laser ranging interfer-
362 ometer for Earth science applications?, *Surv. Geophys.*, *37*(2), 453-470

- 363 Folland, C., T. Karl, J. Christy, R. Clarke, G. Gruza, J. Jouzel, M. Mann, J. Oerlemans,
364 M. Salinger, and S.-W. Wang, Observed climate variability and change, In: Houghton,
365 J. et al. (eds.), *Climate Change 2001: The Scientific Basis*, *Cambridge Univ. Press*,
366 99-181
- 367 Forootan, E., R. Rietbroek, J. Kusche, M. Sharifi, J. Awange, M. Schmidt, P. Omondi,
368 and J. Famiglietti (2014), Separation of large-scale water storage patterns over Iran
369 using GRACE, altimetry and hydrological data, *Remote Sens. Environ.*, *140*, 580-595
- 370 Houborg R., M. Rodell, B. Li, R. Reichle, and B. Zaitchik, Drought indicators based
371 on model-assimilated Gravity Recovery and Climate Experiment (GRACE) terrestrial
372 water storage observations, *Water Resour. Res.*, *48*, W07525
- 373 Humphrey, V., L. Gudmundsson, and S. Seneviratne (2016), Assessing global water stor-
374 age variability from GRACE: Trends, seasonal cycle, subseasonal anomalies and ex-
375 tremes, *Surv. Geophys.*, *37*, 357-395
- 376 Huntington, T. (2006), Evidence for intensification of the global water cycle: Review and
377 synthesis, *J. Hydrol.*, *319*, 83-95
- 378 Hosking, J.R.M. (1985), Maximum likelihood estimation of the parameters of the gener-
379 alized extreme value distribution, *Appl. Stat.*, *34*, 301-310
- 380 Landerer, F., and S. Swenson (2012), Accuracy of scaled terrestrial water storage esti-
381 mates, *Water Resour. Res.*, *48*, W04531
- 382 Martins, E.S., and J.R. Stedinger (2000), Generalized maximum-likelihood generalized
383 extreme value quantile estimators for hydrologic data, *Water Resour. Res.*, *36*(3), 737-
384 744.

- 385 Moore, P., and S. Williams (2014), Integration of altimetric lake levels and GRACE
386 gravimetry over Africa: Inferences for terrestrial water storage change 2003-2011, *Water*
387 *Resour. Res.*, *50*(12), 9696-9720
- 388 Phillips, T., R. Nerem, B. Fox-Kemper, J. Famiglietti, and B. Rajagopalan (2012), The
389 influence of ENSO on global terrestrial water storage using GRACE. *Geophys. Res.*
390 *Lett.*, *39*(16), L16705.
- 391 Rietbroek, R., S.-E. Brunnabend, J. Kusche, J. Schröter, and C. Dahle (2016), Revisiting
392 the contemporary sea level budget on global and regional scales, *Proc. Nat. Acad. Sci.*
393 *U.S.A.*, *113*(6), 15041509.
- 394 Seoane, L., G. Ramillien, F. Frappart, and H. Leblanc (2013), Regional GRACE-based
395 estimates of water mass variations over Australia: validation and interpretation, *Hydrol.*
396 *Earth Syst. Sci.*, *117*, 4925-4939.
- 397 Springer, A., J. Kusche, K. Hartung, C. Ohlwein, and L. Longuevergne (2014), New
398 estimates of variations in water flux and storage over Europe based on regional (Re)
399 analyses and multisensor observations, *J. Hydrometeorol.*, *15*(6), 23972417.
- 400 Stedinger, J., R. Vogel, and E. Foufoula-Georgiou (1992), Frequency analysis of extreme
401 events, In: Maidment, R. (ed.) *Handbook of Hydrology McGraw-Hill*, New York, NY
- 402 Ogawa, R., B. F. Chao, and K. Heki (2011), Acceleration signal in GRACE time-variable
403 gravity in relation to interannual hydrological changes, *Geophys. J. Int.*, *184*(2), 673679.
- 404 Velicogna, I., T. Sutterley, and M. van den Broeke (2014), Regional acceleration in ice
405 mass loss from Greenland and Antarctica using GRACE time-variable gravity data,
406 *Geophys. Res. Lett.*, *41*(22), 8130-8137.

Table 1. Differences

of one-in-five year levels from ERA-Interim and simulated GRACE/GRACE-FO derived TWF

with respect to ERA-Interim, 1983.0-2015.0 (latitude-weighted land-only RMS, m/mon)				
		ERA-I	GRACE/GRACE-FO	GRACE/GRACE-FO
	years	vs. 1983.0-2015.0	vs. ERA-I 1983.0-2015.0	vs. ERA-I, same timeframe
2007.0-2015.0	8.0	0.012	0.015	0.011
2003.0-2015.0	12.0	0.009	0.012	0.009
1999.0-2015.0	16.0	0.008	0.011	0.009
1991.0-2015.0	24.0	0.004	0.008	0.008
1983.0-2015.0	32.0	-	0.007	0.007

407 Yoon, J.-H., S. Wang, R. Gilles, B. Kravitz, L. Hipps, and P. Rasch (2015), Increasing
 408 water cycle extremes in California and in relation to ENSO cycle under global warming,
 409 *Nat. Commun.*, 6:8657, doi:10.1038/ncomms9657.

Figure 1. (a) One-in-five-year levels of anomalously high total water storage (TWS) with respect to climatology, as observed by the GRACE satellite mission (2003.0-2015.0), (b) one-in-five-year levels of anomalously low TWS from GRACE, (c, e, g and j) TWS time series for locations indicated by red circles) (d and h) corresponding empirical and fitted probability density functions for anomalously high TWS, (f and j) corresponding empirical and fitted probability density functions for anomalously low TWS. c and d: Central Amazon, g and h: Parana, e and f: Cuvelai-Etosha, i and j: Northern Australia

Figure 2. (a) One-in-five-year levels of anomalously high total water flux (TWF) as observed by the GRACE satellite mission (2003.0-2015.0), (b) one-in-five-year levels of anomalously low TWF from GRACE, (c) one-in-five-year levels of anomalously high TWF from ERA-Interim reanalysis, (d) one-in-five-year levels of anomalously low TWF from ERA-Interim reanalysis

Figure 3. (a) One-in-five-year levels of anomalously high TWF from ERA-Interim, 2003.0-2015.0, (b) same, from simulated GRACE data (ERA-Interim plus GRACE correlated noise model), 2003.0-2015.0, (c) one-in-five-year levels of anomalously high TWF from ERA-Interim, 1991.0-2015.0, (d) same, from simulated GRACE data (ERA-Interim plus GRACE correlated noise model), 1991.0-2015.0, (e) one-in-five-year levels of anomalously high TWF from ERA-Interim, 1983.0-2015.0, (f) same, from simulated GRACE data (ERA-Interim plus GRACE correlated noise model), 1983.0-2015.0

Figure 1. Figure

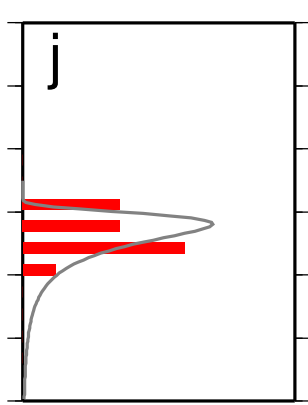
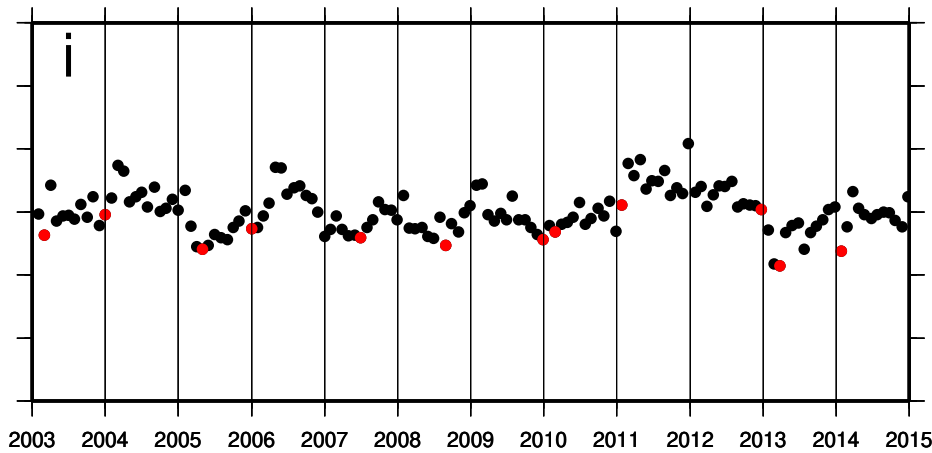
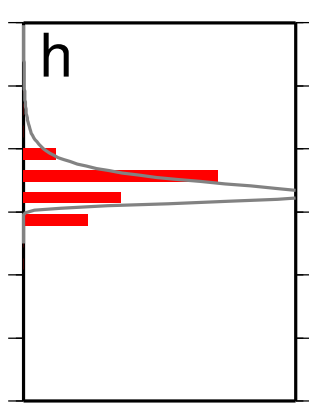
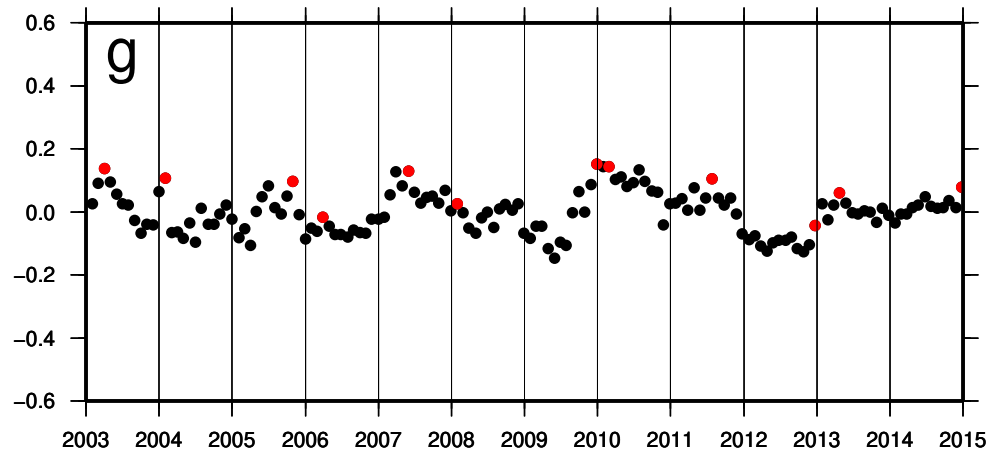
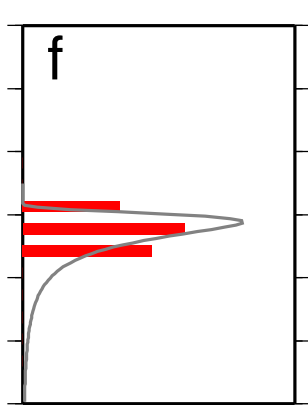
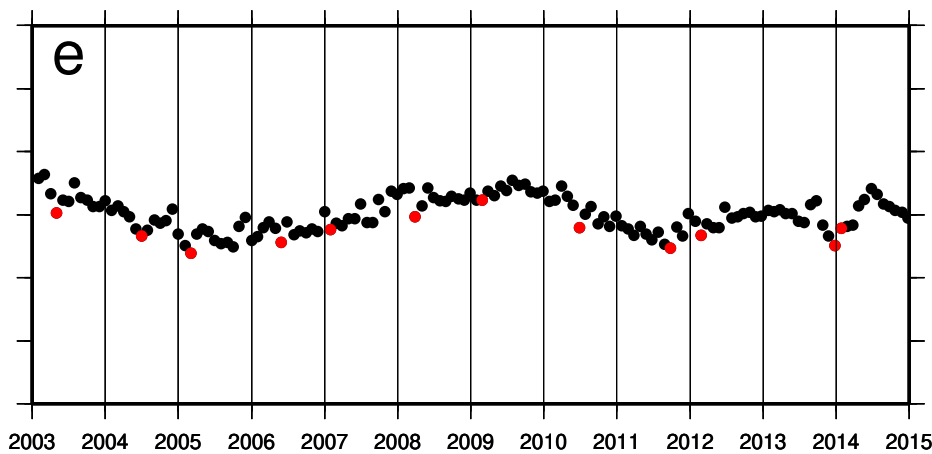
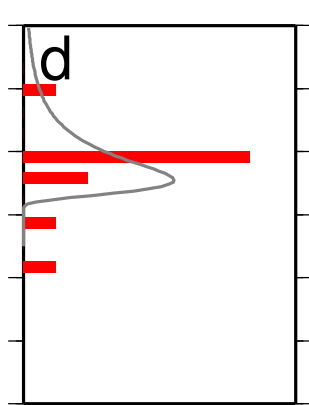
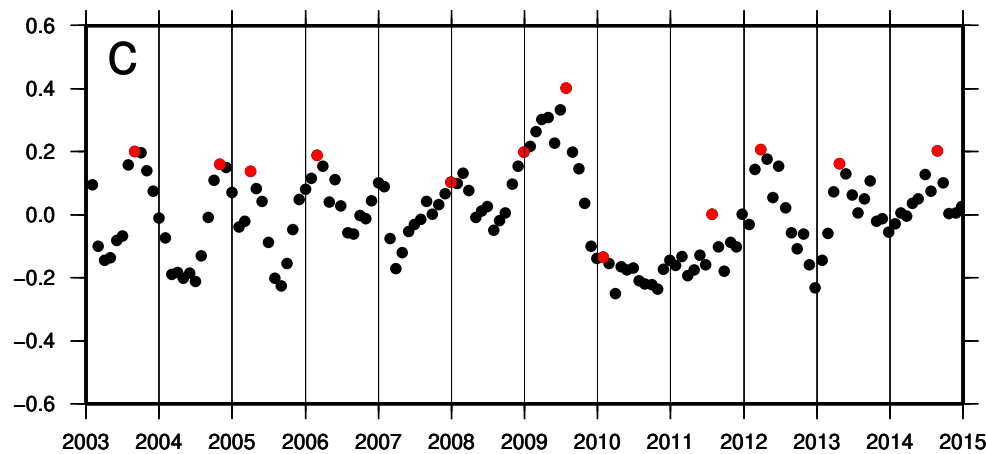
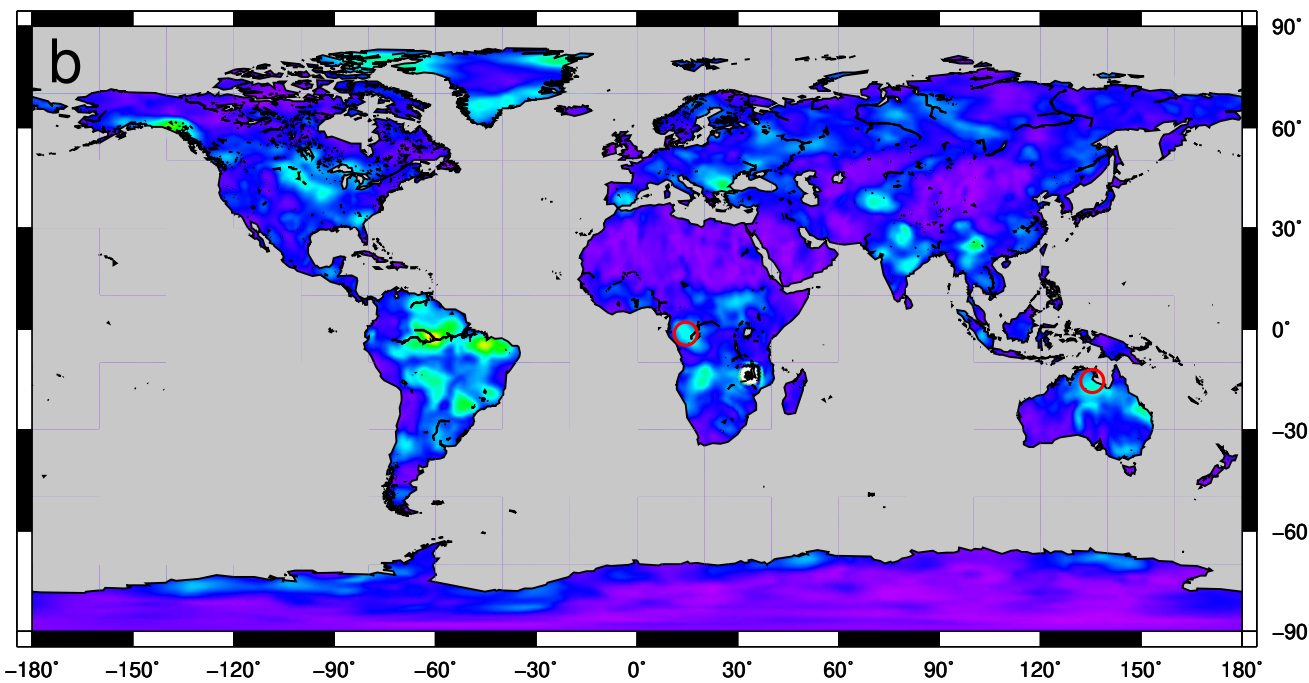
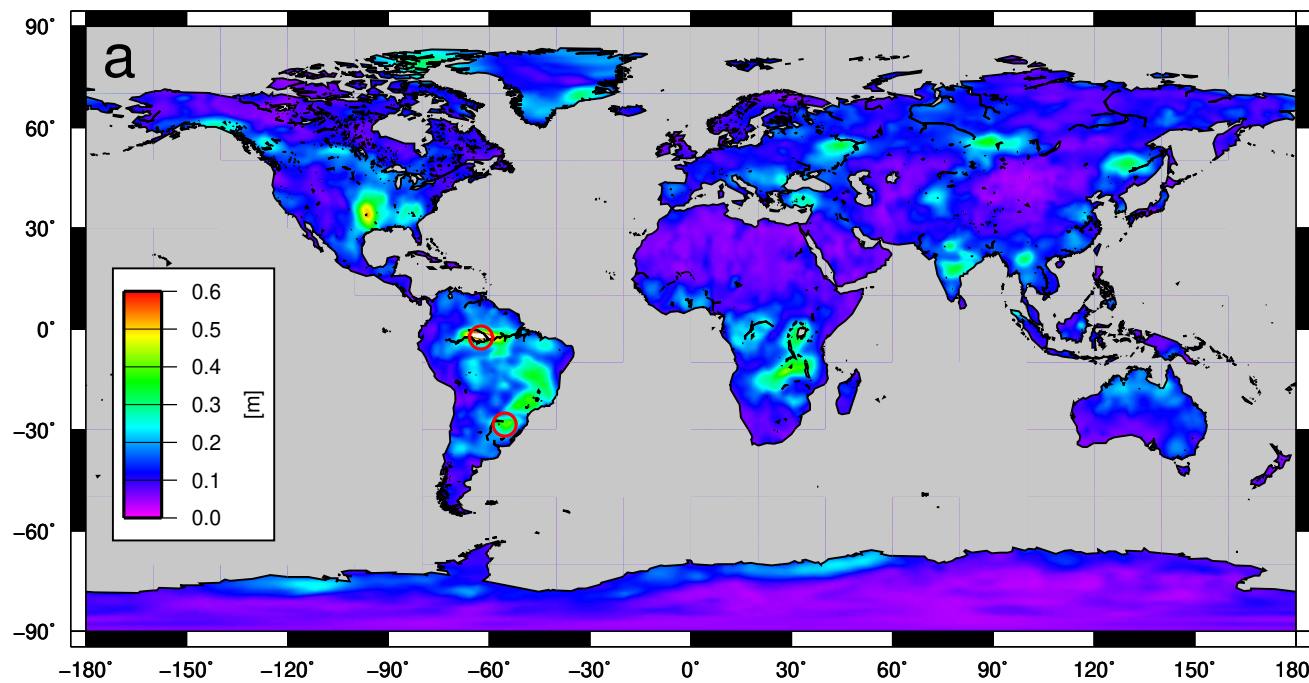


Figure 2. Figure

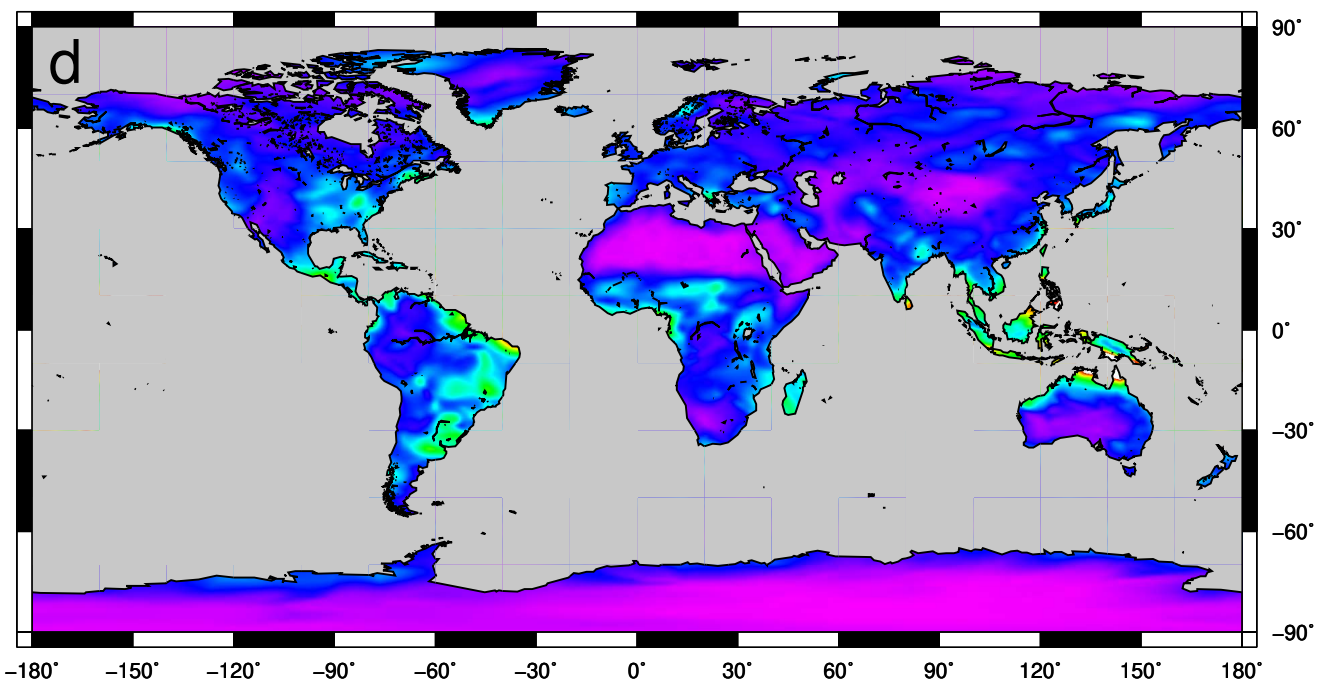
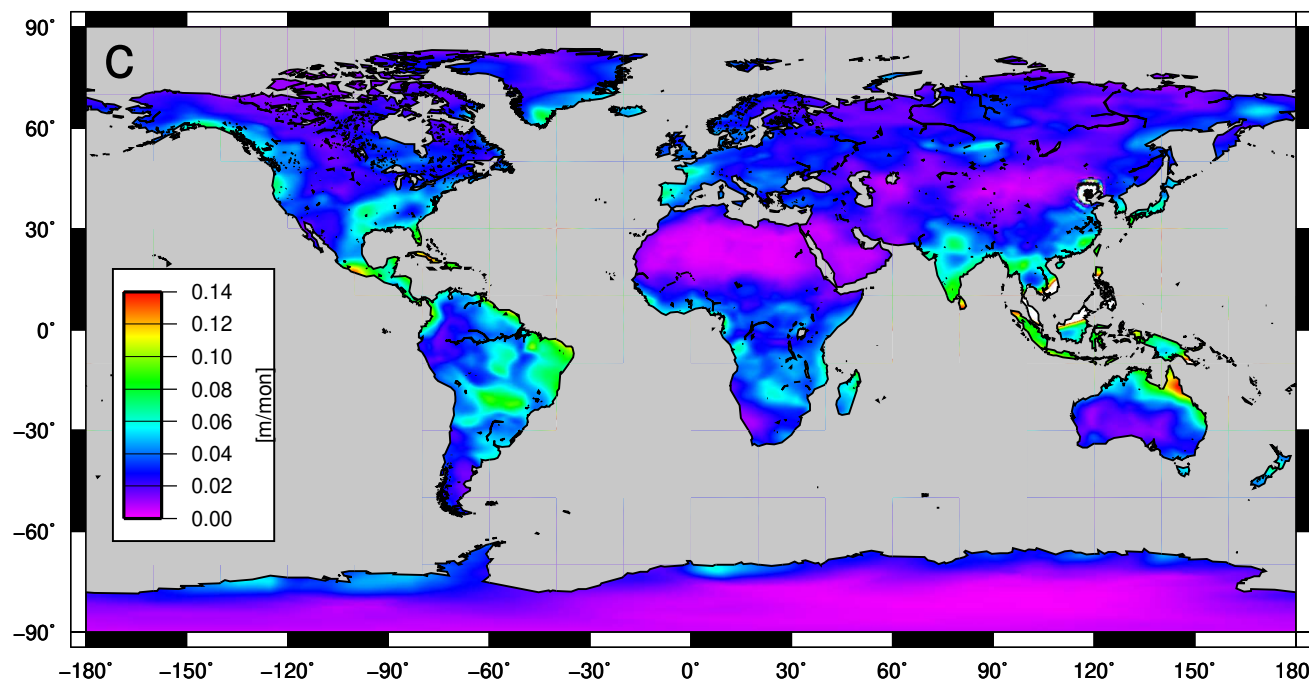
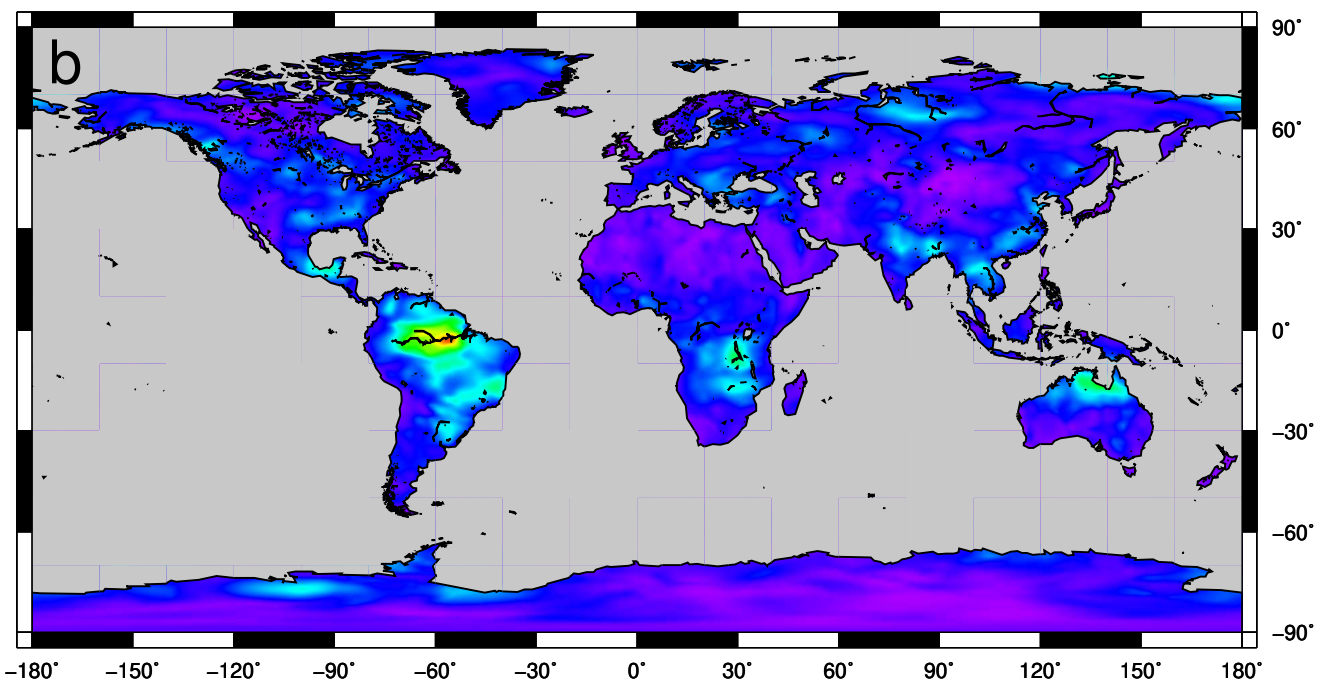
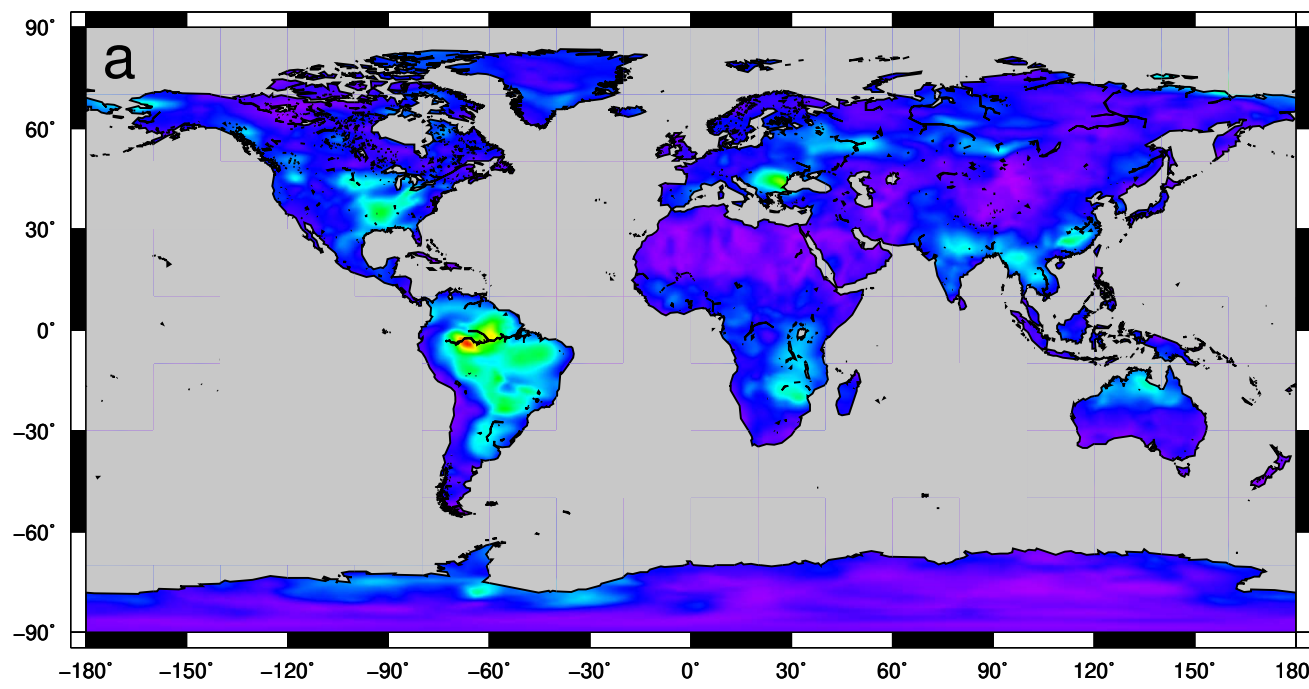


Figure 3. Figure

